frontiers | Frontiers in Environmental Science

TYPE Original Research
PUBLISHED 04 September 2025
DOI 10.3389/fenvs.2025.1658113

OPEN ACCESS

EDITED BY
Juergen Pilz,
University of Klagenfurt, Austria

REVIEWED BY
Guangxuan Wang,
Vrije University Brussels, Belgium
Yazhou Zhao,
Tongji University, China
Muhammad Sajjad,
Iqra National University, Pakistan

*CORRESPONDENCE
Qianrong Zhang,
zqrong1@cdtu.edu.cn

†These authors have contributed equally to this work and share first authorship

RECEIVED 02 July 2025
ACCEPTED 06 August 2025
PUBLISHED 04 September 2025

CITATION
He J, Wang S, Zhong B and Zhang Q (2025) Photovoltaic power generation spatial planning and carbon emission reduction benefit assessment based on integrated model: a case study of Qinghai province.
Front. Environ. Sci. 13:1658113.
doi: 10.3389/fenvs.2025.1658113

Photovoltaic power generation spatial planning and carbon emission reduction benefit assessment based on integrated model: a case study of Qinghai province

Junjie He[1†], Simin Wang[1†], Boyang Zhong[1†] and Qianrong Zhang[2*]

[1]School of Automotive and Transportation, Chengdu Technological University, Chengdu, China, [2]College of Big Data and Artificial Intelligence, Chengdu Technological University, Chengdu, China

As an important source of clean energy, the Photovoltaic (PV) industry still requires in-depth research to optimize its development space and maximize carbon emission reduction benefits. This study takes Qinghai Province as the research area, integrating topographical, climatic, and economic factors to establish a Photovoltaic suitability evaluation system encompassing 15 indicators. Subsequently, the spatial distribution of feasible development zones was assessed, taking into account various constraints. Then, the binary local Moran's I index method was used to analyze its spatial coupling relationship with electricity consumption. Finally, the benefits of carbon emission reductions were quantified. The results indicate that approximately 52.61% of Qinghai Province is considered to be an area with development potential, with a spatial distribution characterized by three belts and two areas. Meanwhile, there is a significant correlation between Photovoltaic power generation potential and electricity demand. It is predicted that by 2030, Qinghai Province's electricity consumption will reach 1.235×10^{12} kwh. To achieve a balance between supply and demand, it will be necessary to construct approximately 18,849.35 km^2 of Photovoltaic power generation facilities, which are expected to reduce carbon dioxide emissions by 9.48×10^8t annually. This study provides scientific basis for the optimized development of the Photovoltaic industry, helping to achieve regional energy transition and carbon emission reduction targets, and promoting sustainable development.

KEYWORDS

combination empowerment, suitability, photovoltaic potential area, moran's I, carbon emission reduction

1 Introduction

With the intensification of climate change and the energy crisis, the development of clean energy has become an inevitable direction for future development (Sahu, 2015). To address global warming, the international community has established important legal documents such as the United Nations Framework Convention on Climate Change (UNFCCC) and the Paris Agreement, promoting global cooperation to reduce carbon

emissions, drive green transformation, and collectively achieve carbon neutrality goals (Mitchell et al., 2018) Under the guidance of China's 'dual carbon' objectives, PV energy is rapidly emerging as one of its primary energy sources. China possesses abundant solar energy resources, with approximately 66.8% of its land area receiving solar radiation exceeding 5,040 MJ/m^2 annually (Tong et al., 2025). As of the end of February 2025, the country's total installed power generation capacity reached 340 million kilowatts, representing a year-on-year increase of 14.5%. Among this, solar power generation capacity stood at 93 million kilowatts, marking a year-on-year increase of 42.9% (National Energy Administration, 2025; National Energy Administration, 2014)

The current research boom in PV power generation is primarily reflected in two areas of in-depth exploration: (1) research into ways to optimize the power generation efficiency of PV systems and discussions on factors affecting PV power generation (Yuan et al., 2019; Antonanzas et al., 2018; Mahmud et al., 2021; Jerez et al., 2015; Sharadga et al., 2020); (2) the improvement of regional resource suitability assessment systems and the assessment of PV power generation potential (Zhao et al., 2023; Tan et al., 2025; Ghosh et al., 2023; Yang et al., 2019; Yue et al., 2024; Feng et al., 2025; Zhao et al., 2014; Gholami et al., 2020; Ghosh et al., 2023).

In the early stages of research on the suitability and potential of PV power generation, some studies overemphasized solar energy potential while neglecting factors such as terrain and cost (Song et al., 2023), leading to increased complexity in project planning and construction. Jiawei Wu et al. (2023) approached the issue from three aspects: technical installed capacity, development potential, and cost. They combined long-term meteorological data, EOF analysis, and spatial clustering analysis to assess the development potential of wind and solar power resources in China's desert and Gobi regions, and conducted a suitability evaluation from six aspects: wind and solar resource endowment, socio-economic development, desertification severity, base construction, and grid and road infrastructure. Yushchenko and Alisa's team (Yushchenko et al., 2018) estimated the geographical and technical potential of solar power generation in rural West African regions based on terrain, legal and social constraints, and factors that may promote or hinder the development of solar power generation. However, comprehensive studies considering multiple factors such as geography, cost, climate, and policy remain insufficient. Therefore, establishing a targeted and robust indicator system is crucial for ensuring the scientific validity and effectiveness of PV suitability assessments (Amrani et al., 2023).

In PV suitability assessment studies, the scientific and rational determination of factor weighting methods directly impacts the accuracy and reliability of assessment results, making it a critical step in ensuring the scientific soundness of site selection decisions. Existing research has made some progress in weighting determination methods: Elboshy et al., 2022) utilized the GIS-AHP framework to rank the weights of 10 indicators across four major categories—location, environment, meteorology, and climate—to construct a photovoltaic land suitability index. He then mapped the suitability of sites for photovoltaic power plants in Egypt, providing decision-making support for the strategic layout of renewable energy projects. Dongchuan Wang et al. (2023) proposed an assessment framework combining subjective and objective approaches, integrating the subjective experiential judgements of AHP with the objective data-driven characteristics of the CRITIC method to achieve a multi-dimensional evaluation of PV power plant site suitability. However, current weight determination methods still have obvious limitations: on the one hand, existing methods struggle to effectively balance the differences between expert subjective judgements and objective data, and lack systematic consideration of uncertainties in the evaluation process; on the other hand, they fail to adequately consider the decision preferences of various stakeholders, leading to weight allocation that cannot optimally coordinate the interests of multiple parties. Therefore, developing a comprehensive weight determination method that balances expert experience, data objectivity, uncertainty quantification, and multi-party interest coordination remains an important research direction for enhancing the scientific rigor and reliability of PV suitability evaluations.

Energy companies and local governments are increasingly focusing on the dual economic and ecological benefits of integrated PV power stations. Using geographic information systems (GIS) to create site suitability maps can provide important support for policymakers, especially since accurate PV power generation forecasts are crucial for developing new energy development plans (Chen et al., 2023). To achieve the goal of reducing greenhouse gas emissions by 55% by 2030, the European Union is accelerating the construction of PV power plants and has set a target to significantly increase PV installed capacity to 455–605 GW (Li et al., 2021). However, in some regions, excessive energy supply relative to demand has led to severe PV curtailment (O'Shaughnessy et al., 2020). Therefore, it is urgent to further explore the spatial mismatch between PV power generation and electricity consumption to improve energy efficiency and optimize resource allocation (Yang and Huang, 2023).

China is a vast country with significant variations in climate and terrain, resulting in distinct regional and differentiated characteristics in PV suitability studies across different regions. Dongchuan Wang (Wang et al., 2023)and colleagues utilised remote sensing data and multi-source information to conduct a detailed analysis of the feasibility and potential of PV power generation on the Qinghai-Tibet Plateau; Yazhou Zhao (Zhao et al., 2024) and colleagues, through a comprehensive study of six northwestern provinces, conducted a comprehensive assessment of the PV suitability of the region. However, existing studies have certain scale limitations. Therefore, conducting a systematic, comprehensive, and detailed assessment of PV power generation potential, analysing regional differences, and quantifying carbon emission reduction benefits based on previous research can provide strong support for government decision-making, promote the rational development of PV resources, provide scientific basis for enterprise site selection, and further assess and optimize regional carbon emission reduction benefits.

Therefore, to address the above issues, this paper takes Qinghai Province as the research object and comprehensively explores the spatial distribution of PV power generation and its CO_2 emission reduction benefits, specifically including the following content:

1. Comprehensively evaluating the suitability of land use for the PV industry: Taking into account various factors affecting the suitability of PV power generation, such as basic geography, construction costs, and climate, this study combines the

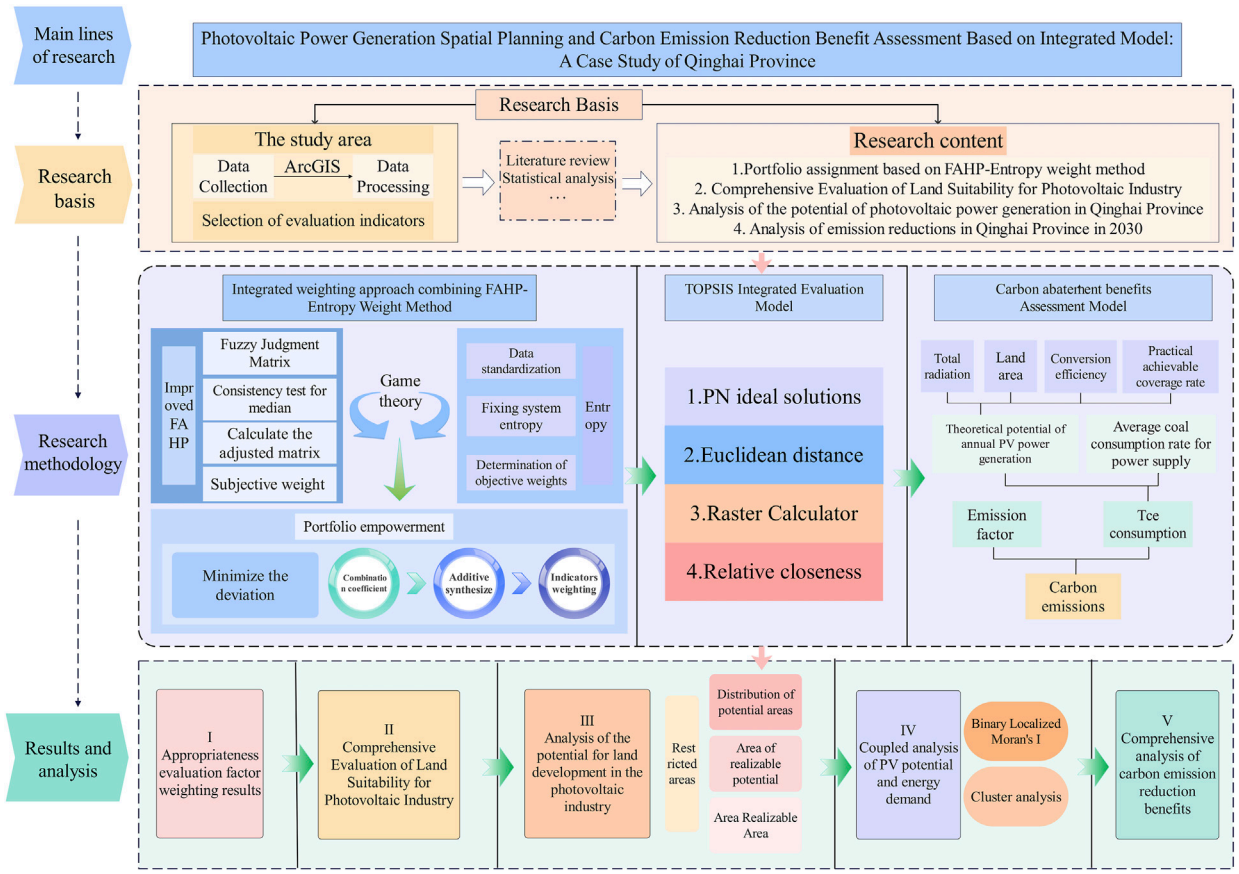

FIGURE 1
Research roadmap.

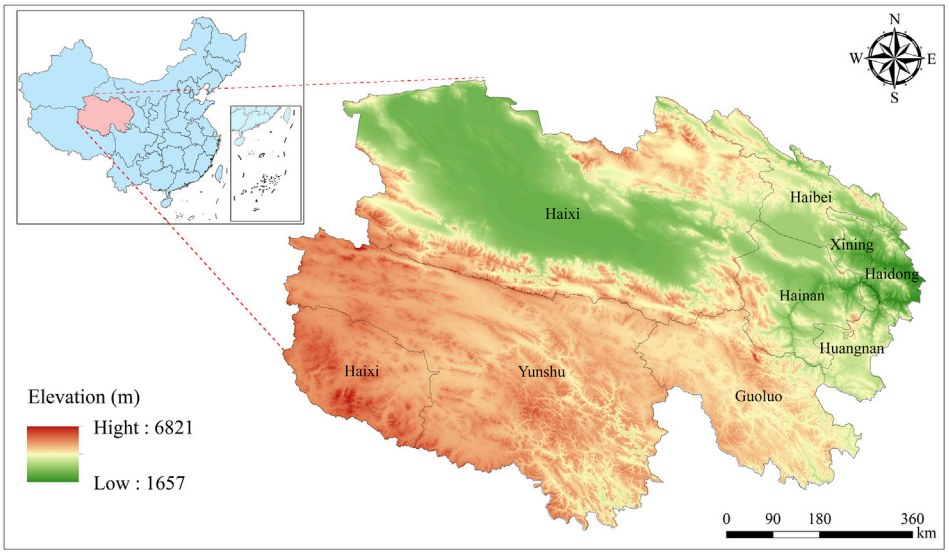

FIGURE 2
Study area–Qinghai Province, China.

FAHP-entropy weighting method based on game theory with the TOPSIS method to construct a comprehensive evaluation model for the suitability of land use for the PV industry.

2. PV power generation potential and the relationship between electricity supply and demand: Combining national requirements and the current status of PV development in Qinghai Province, this study further explores the spatial distribution of PV potential in Qinghai Province and analyzes the supply-demand relationship between PV potential and electricity consumption using the binary local Moran's I method.
3. Assessment of carbon emission reduction benefits: Based on the achievable potential of PVs, further estimates of Qinghai Province's theoretical power generation potential and CO_2 emission reduction benefits were made.

The framework of this paper is shown in Figure 1.

2 Materials and methods

2.1 Research area

Figure 2 shows the topographic map of Qinghai Province. Qinghai Province is located in northwestern China, with geographical coordinates of 89°35′–103°04′east longitude and 31°36′–39°19′north latitude. It spans approximately 1,200 km from east to west and 800 km from north to south, covering a total area of 722,300 square kilometers, accounting for one-thirteenth of China's total land area and ranking fourth in size. The province borders Gansu, Sichuan, Xinjiang, and Tibet, serving as a vital link connecting Tibet, Xinjiang, and the rest of the country. Qinghai is deeply embedded in the Qinghai-Tibet Plateau, featuring a highland continental climate. It receives strong solar radiation with prolonged sunlight, with annual radiation totals ranging from 5,860 to 7,400 MJ per square metre, and annual sunshine hours between 2,336 and 3,341 h (Qinghai Provincial People's Government, 2025) The province boasts abundant solar energy resources and significant development potential.

2.2 Data sources and processing

Terrain data includes elevation data, land use data, and water body and water network data. Elevation data is sourced from the Geospatial Data Cloud, utilizing the SRTM 3″(≈90 m) DEM. According to Zhang, K.et al., the local relative vertical accuracy (RMSE) of SRTM is approximately 3.8–4.8 m, with a 90% confidence linear error (LE90) less than 7 m, demonstrating that it typically outperforms 10 m in typical regions (Zhang et al., 2019).

Land use data is sourced from the Zenodo platform (GaryBikini, 2023), which is based on the Google Earth Engine platform. Using imagery data, it has constructed a 2022 land cover dataset (CLCD) with a resolution of 30 m × 30 m, offering high spatial accuracy. Water body and water network data is sourced from OpenstreetMap (OSM), with data accessed on 14 March 2025, ensuring strong timeliness and accuracy.

The resource climate data includes solar radiation, average temperature, surface temperature, sunshine duration, 10-m wind speed, precipitation, and relative humidity, all sourced from the National Qinghai-Tibet Plateau Scientific Data Center (TPDC) (Feng and Wang, 2020; Zhang and Peng, 2024.). The solar radiation data is based on ISCCP-HXG cloud products and combined with sunshine duration data from 2,261 meteorological stations, using a geographically weighted regression method for inversion, with accuracy superior to other global data products. The remaining meteorological data are based on daily observations from 699 meteorological stations in China, generated using thin-plate spline and random forest interpolation methods. The data have been validated through comparisons with independent observation data and existing products (such asCMFD、HRLT), and the results indicate that the data have high reliability and can effectively support climate research in fields such as ecology, hydrology, and agriculture.

Economic data includes railway, first-class, second-class, and third-class roads, as well as urban point locations and nighttime lighting remote sensing data. Railway, road, and urban settlement data are sourced from OpenStreetMap (OSM), with data accessed on 14 March 2025, ensuring strong timeliness. Among these, first-level roads include expressways and their connecting roads, as well as trunk roads and their connecting roads; second-level roads encompass main roads, secondary roads, and their connecting roads, as well as residential area roads; third-level roads include rural roads, small roads, bicycle paths, and their connecting roads. Nighttime lighting remote sensing data is sourced from the National Qinghai-Tibet Plateau Science Data Center (Zhang et al., 2024). Based on an assessment of the nighttime lighting data, the coefficient of determination (R^2) reaches 0.95, and the pixel-level linear slope is 0.99, indicating high data quality.

The remaining data includes the spatial distribution of solar panels in China in 2022, nature reserves in Qinghai Province, China's administrative divisions, and electricity consumption data for Qinghai Province. The spatial distribution data for solar panels is sourced from the National Qinghai-Tibet Plateau Scientific Data Center (Lü et al., 2024). This dataset is based on the Google Earth Engine platform and employs a combination of hierarchical sampling and zone-based modeling, with interpretation and generation performed using a random forest algorithm. The dataset achieves an F1-score exceeding 0.92, indicating high accuracy. The data on nature reserves in Qinghai Province is sourced from the Zhongke SuperMap Geographic Cloud Platform - Data Resource Center (https://www.zkchaotu.com). This dataset is based on the lists of nature reserves and functional zoning maps published by Qinghai Province's environmental protection, forestry, agriculture, and land management departments, and collects baseline data on national-level nature reserves as of January 2018. The data was produced through high-resolution satellite imagery and geographic registration. China's administrative division data is sourced from Zenodo (Yang et al., 2019) which has reliable regional divisions. Qinghai Province's electricity consumption data is sourced from the National Bureau of Statistics (https://data.stats.gov.cn), which provides authentic and reliable data.

This paper integrates long-term sequence data and high spatial resolution data from multiple sources. ArcGIS is used to convert the

TABLE 1 Data sources.

Data name	Data type	Data source	Data time
Solar radiation	Raster	National Qinghai-Tibet Plateau Scientific Data Center	2010-2017
Surface temperature	Raster	National Qinghai-Tibet Plateau Scientific Data Center	2020
Air temperature	Raster	National Qinghai-Tibet Plateau Scientific Data Center	2020
Sunshine hours	Raster	National Qinghai-Tibet Plateau Scientific Data Center	2020
Wind speed at 10 m	Raster	National Qinghai-Tibet Plateau Scientific Data Center	2020
Precipitation	Raster	National Qinghai-Tibet Plateau Scientific Data Center	2020
Relative humidity	Raster	National Qinghai-Tibet Plateau Scientific Data Center	2020
Elevation data	Vector	Geospatial Data Cloud	2020
Urban locations	Vector	OpenStreetMap	2025
Railways	Raster	OpenStreetMap	2025
Night-time lighting	Raster	National Qinghai-Tibet Plateau Scientific Data Center	2020
Land use	Vector	Zenodo	2022
Primary roads	Vector	OpenStreetMap	2025
Secondary roads	Vector	OpenStreetMap	2025
Tertiary roads	Vector	OpenStreetMap	2025
Photovoltaic panel locations	Vector	National Qinghai-Tibet Plateau Scientific Data Center	2022
Nature reserve locations	Vector	Zhongke Super Map Geography Cloud Platform	2018
Water bodies and water networks	Vector	OpenStreetMap	2025
Administrative divisions	Vector	Zenodo	2023
Electricity consumption	Numerical	National Bureau of Statistics	2005-2023

geographic coordinate system of the raw data into a projected coordinate system. All data is pre-processed at a spatial resolution of 90 m to ensure the accuracy and effectiveness of subsequent spatial analysis. Specific operations are shown in Table 1.

2.3 Selection of suitability evaluation indicators

The selection of sites for PV power stations is influenced by a variety of factors. This paper combines domestic and international research findings to construct a suitability evaluation index system for PV land development in Qinghai Province. The system consists of three criteria layers: basic geography, resource climate, and development costs. The specific indicators are shown in Table 2 below.

2.3.1 Basic geographical conditions

Basic geographical conditions include slope gradient, slope aspect, and land use type. Large-scale PV power plants require relatively flat areas (Luan et al., 2021). Excessively steep slopes make the construction of PV power plants more challenging. Many studies in China have set an upper limit for slope gradients below a certain angle (Fang et al., 2018). Therefore, this study analyzed elevation

TABLE 2 Selection of suitability evaluation factors.

Level 1 indicator	Level 2 indicator	Unit
Resource climate conditions	Solar radiation	W/m^2
	Sunshine hours	h
	Precipitation	mm
	Air temperature	K
	Average wind speed at 10 m	m/s
	Relative humidity	%
	Surface temperature	K
Basic geographical conditions	Slope	°
	Slope aspect	-
	Land use	-
Development cost conditions	Distance from primary road	km
	Distance from secondary road	km
	Distance from tertiary road	km
	Distance from town	km
	Distance from railway	km

data using ArcGIS's surface analysis tools to calculate slope gradient and slope aspect data. According to national policies, land use type is an important restrictive factor in PV land development. For example, land types such as farmland are prohibited development zones for PV land use (Ministry of Natural Resources, 2024)

2.3.2 Resource climate conditions

Resource climate conditions include solar radiation, sunshine hours, air temperature, 10-m wind speed, surface temperature, relative humidity, and precipitation. Among these, solar radiation is the core factor for PV power generation, and regions with abundant solar radiation are more suitable for PV power generation. Experts in this field generally agree that solar radiation is an important indicator for assessing the potential of PV power generation (Zhang et al., 2016). Sunshine hours are also an important standard for measuring PV power generation (OpenStreetMap contributors, 2025). In the climate dimension, this study simultaneously incorporates solar radiation and sunshine duration into the evaluation. Solar radiation determines the total energy available per unit area, while sunshine duration describes the effective duration of sunlight exposure. Although these two indicators are correlated, they are not collinear—regression analysis of monthly data from 69,000 stations worldwide still yields significant residuals, indicating that sunshine duration contains independent information beyond solar radiation (Suehrcke et al., 2013). Additionally, recent multi-criteria site selection studies have also set both as the highest-weighted climate factors. (de Luis-Ruiz et al., 2024). Therefore, retaining the combination of solar radiation and sunshine duration avoids omitting critical information. Air temperature affects the performance of PV modules, with high temperatures potentially leading to a decrease in module efficiency. Wind speed influences heat dissipation; appropriate wind speeds can lower module temperatures and improve efficiency, while also removing some dust adhering to PV panels and reducing the cost of manual dust cleaning. Humidity and precipitation can lower module temperatures, enhance power generation efficiency, and aid in evaluating PV power generation potential, while also cleaning modules and improving the ecological environment.

2.3.3 Development cost conditions

Development cost conditions include distance from towns, distance from railways, and distance from roads (first, second, and third class). Different road types and distances affect the construction of PV power stations and the transportation costs of subsequent maintenance. Therefore, roads are classified into different grades (OpenStreetMap contributors, 2025) for subsequent processing and analysis.

2.4 Research methods

2.4.1 Game theory-based FAHP--entropy weight method of portfolio assignment

2.4.1.1 FAHP

In terms of subjective assignment, the traditional hierarchical analysis method (AHP) relies on precise expert scoring, while the actual scoring often has uncertainty. Fuzzy hierarchical analysis (FAHP) effectively solves this problem by introducing triangular fuzzy numbers to replace the point value scoring, which can better characterize the ambiguity of decision-making (Xu et al., 2023) and realize the index sorting and weight determination through fuzzy number comparison (Liu et al., 2023).

However, the traditional FAHP may lead to a weight calculation result of 0 under certain circumstances. Sui Minggang and Wei Weight (Sui and Wei, 2000) improved the method and effectively overcame this defect. The steps of the improved FAHP calculation are as follows:

Step 1: Constructing a fuzzy judgment matrix.

Combining the evaluation object and evaluation indexes, the fuzzy judgment matrix A is derived as $A = (a_{ij})_{n\times n}$,included among these $a_{ij} = [l_{ij}, m_{ij}, u_{ij}]$,is a closed interval with m_{ij} as the median.

Step 2: Consistency test for the median matrix M.

After calculating the maximum eigenvalue $\lambda_{\max}$ of the median matrix M, in order to assess the reasonableness of the judgment matrix, the consistency test of the matrix is performed in this paper. The consistency ratio CI is calculated first, as in Equation 1. Subsequently, the value of CR is calculated, $CR = CI/RI$ and the matrix consistency test is passed if $CR < 0.1$ time. Otherwise, the judgment value needs to be adjusted.

$$CI = \frac{\lambda_{\max} - n}{n-1} \tag{1}$$

Step 3: Construct fuzzy judgment factor matrix.

A fuzzy judgment factor matrix is constructed for the judgment matrix as in Equation 2:

$$E = (e_{ij})_{n\times n} = \begin{bmatrix} 1 & 1-(u_{12}-l_{12})/2m_{12} & \cdots & 1-(u_{1n}-l_{1n})/2m_{1n} \\ 1-(u_{21}-l_{21})/2m_{21} & 1 & \cdots & 1-(u_{2n}-l_{2n})/2m_{2n} \\ \vdots & \vdots & \vdots & \vdots \\ 1-(u_{n1}-l_{n1})/2m_{n1} & 1-(u_{n2}-l_{n2})/2m_{n2} & \cdots & 1 \end{bmatrix} \tag{2}$$

Where $e_{ij} = (u_{ij} - l_{ij})/2m_{ij}$, the standard deviation value, is used to reflect the fuzzy level of expert judgment. The higher the fuzzy level of the indicator assignment result, the lower its credibility; conversely, the higher the credibility.

Step 4: Computation of the adjustment judgment matrix Q

$$Q = M \times E = \begin{bmatrix} m_{11} & m_{12} & \cdots & m_{1n} \\ m_{21} & m_{22} & \cdots & m_{2n} \\ \vdots & \vdots & \vdots & \vdots \\ m_{n1} & m_{n2} & \cdots & m_{nn} \end{bmatrix} \times \begin{bmatrix} 1 & 1-(u_{12}-l_{12})/2m_{12} & \cdots & 1-(u_{12}-l_{12})/2m_{12} \\ 1-(u_{12}-l_{12})/2m_{12} & 1 & \cdots & 1-(u_{12}-l_{12})/2m_{12} \\ \vdots & \vdots & \vdots & \vdots \\ 1-(u_{12}-l_{12})/2m_{12} & 1-(u_{12}-l_{12})/2m_{12} & \ldots & 1 \end{bmatrix} \tag{3}$$

Where M refers to the median matrix whose constituent elements are the median values corresponding to the triangular fuzzy numbers.

Step 5: Convert the judgment matrix Q to a judgment matrix Q' with diagonal 1.

Step 6: Calculate the weight of each indicator using the square root method.

Calculate the number of fuzzy numbers per line for the geometric mean, and then normalize the geometric mean as in Equation 4:

$$\omega_i = \frac{\bar{\omega}_i}{\sum_{i=1}^{n}\left(\prod_{j=1}^{n} a_{ij}\right)^{\frac{1}{n}}},\ i = 1, 2, ..., n \tag{4}$$

This study adopts a three-level hierarchical structure, in which the weights of the indicator level need to be combined with the weights of the criterion level to calculate its global importance. The specific steps are as follows: (1) Calculate the criterion layer weight w_k and the indicator layer relative weight $w_{k|i}$, respectively; (2) The final weight of each indicator in the final indicator layer is: $\omega_i = w_k \times w_{k|i}$. Where w_k denotes the weight of criterion k and $w_{k|i}$ denotes the weight of the ith indicator under criterion k.

2.4.1.2 Entropy weighting

In this study, the entropy weight method is used to determine the weights of indicators. In previous studies, Al-Abadi et al. (2025) used the entropy weight method to objectively assign weights based on the degree of dispersion of sample data, identifying the factors that have the greatest impact on photovoltaic site selection. On this basis, this paper introduces a smoothing correction method to optimize weight distribution in response to the issue of some indicators having entropy values close to 1, resulting in excessively low weights. The steps are as follows:

Step 1: Data standardization.

In order to eliminate the influence of the inter-indicator scale, this paper adopts the 0–1 standardization method to process the data of the selected indicators. Among them, the larger the value of the positive indicators, the better, and vice versa for the reverse indicators, the standardization formula is as follows:

$$x_{ij}^{'} = \frac{\left|x_{ij} - \min(x_i)\right|}{\max(x_i) - \min(x_i)} \tag{5}$$

Where: x_{ij} and $x_{ij}^{'}$ are the indicator data before and after standardization, respectively; $\max(x_i)$ and $\min(x_i)$ are the maximum and minimum values in the indicator data, respectivel.

Step 2: Determine the system entropy.

Calculate the information entropy of the ith metric e_i as in Equation 6:

$$e_i = -\frac{1}{\ln n}\sum_{i=1}^{n} y_i \ln y_i \tag{6}$$

Where: the characteristic weight y_i of the evaluation object under the ith indicator is: $y_i = x_i^{'}/\sum_{i=1}^{n} x_i^{'}$.

The smoothing correction to the entropy value is: $e_i^s = e_i \times (l - s) + s$. In the formula, e_i^s is the entropy value of the corrected indicator i; $s \in [0, 1]$ is the smoothing factor, which controls the degree of entropy correction.

Step 3: Objective weight calculation.

Calculate the weight of the ith indicator:

$$\omega_i = \frac{(1 - e_i^s)}{\sum_{i=1}^{n}(1 - e_i^s)} \tag{7}$$

2.4.1.3 Game theory combinatorial empowerment approach

Step 1: For the L different methods used to determine the weights of n indicators, it can be expressed as:

$$\omega_{li} = (\omega_{l1}, \omega_{l2}, ..., \omega_{\ln}),\ l = 1, 2, ...L \tag{8}$$

Then the linear combination of L weight vectors can be expressed as in Equation 9:

$$\omega = \sum_{l=1}^{L} \alpha_l {\omega_{li}}^{\mathrm{T}}\ (\alpha_l > 0) \tag{9}$$

where ω is the combination weight and α_l is the linear combination coefficient.

Step 2: Based on the game-theoretic combinatorial principle to minimize the ω and ω_l divergence, the objective function can be expressed as in Equation 10:

$$\min\left\|\sum_{l=1}^{L} \alpha_l {\omega_{li}}^{\mathrm{T}} - {\omega_{li}}^{\mathrm{T}}\right\|,\ l = 1, 2, ..., L \tag{10}$$

Step 3: Next, according to the matrix differentiation property, the optimal first order derivative condition of the objective function is as in Equation 11:

$$\sum_{l=1}^{L} \alpha_l \omega_{li} {\omega_{li}}^{\mathrm{T}} = \omega_{li} {\omega_{li}}^{\mathrm{T}},\ l = 1, 2, ...L \tag{11}$$

Step 4: By equating the system of linear equations, calculate $\alpha_l = [\alpha_1, \alpha_2, ...\alpha_L]^{\mathrm{T}}$.

Step 5: Normalization of coefficients as in Equation 12.

$$\alpha_l^{\star} = \frac{|\alpha_l|}{\sum_{i=1}^{L}|\alpha_l|} \tag{12}$$

In Eq. To avoid the possibility of obtaining some negative solutions use the coefficients of the absolute values for normalization.

Step 6: Calculate portfolio weights.

After finding the linear combination coefficients, additive synthesis is performed to calculate the combination weights, a process that makes the data more interpretable. The combination formula is as follows:

$$\bar{\omega}_i = \alpha_1^{\star} \cdot \omega_{1i} + \alpha_2^{\star} \cdot \omega_{2i} \tag{13}$$

2.4.2 TOPSIS integrated evaluation model

TOPSIS is a comprehensive evaluation method based on raw data, which is widely used in multi-indicator decision-making problems by accurately ordering evaluation options. In this paper, based on the improved FAHP-entropy weighting method combined assignment method to calculate the weight of each evaluation index, and combined with the TOPSIS method, the raster calculator in ArcMap is utilized to carry out a comprehensive evaluation of the regions in Qinghai Province. The specific steps are as follows:

Step 1: The graded data were standardized according to the above standardization method, and the standardized data $x_{ij}^{'}$ were obtained for the benefit-type indicator (the larger the better), and the cost-type indicator (the smaller the better), respectively.

Step 2: Determine the positive and negative ideal solutions and the calculation of distance.

Positive and negative ideal solution calculations:

$$V^+ = \left\{\left(\max x_{ij}^{'} | i \in J^+\right), \left(\min x_{ij}^{'} | i \in J^-\right)\right\} = (V_1^+, V_2^+, ..., V_n^+) \quad (14)$$

$$V^- = \left\{\left(\max x_{ij}^{'} | i \in J^-\right), \left(\min x_{ij}^{'} | i \in J^+\right)\right\} = (V_1^-, V_2^-, ..., V_n^-) \quad (15)$$

where is a benefit-based indicator and is a cost-based indicator.

Distance from positive and negative ideal solutions as in Equation 16, 17:

$$D_i^+ = \sqrt{\sum_{i=1}^{n} \varpi_i \left(v_{ij} - V_i^+\right)^2}, \ i = 1, 2, ..., n \quad (16)$$

$$D_i^- = \sqrt{\sum_{i=1}^{n} \varpi_i \left(v_{ij} - V_i^-\right)^2}, \ i = 1, 2, ..., n \quad (17)$$

where V_i^+ and V_i^- are the positive and negative ideal solutions of the ith indicator.

Step 3: Calculate the relative closeness as in Equation 18.

$$C_i = \frac{D_i^-}{D_i^+ + D_i^-}, \ C_i \in [0, 1] \quad (18)$$

where D_i^+ and D_i^- are the distances between the sample indicators and the positive and negative ideal solutions; C_i is the relative closeness, the larger its value the closer it is to the positive ideal solution, and the smaller its value the closer it is to the negative ideal solution.

2.4.3 Quantitative carbon emission reduction assessment models

2.4.3.1 Theoretical potential of PV power generation

The power generation potential of a PV system can be estimated from three key parameters: the total annual solar radiation received per unit area $SR(GWh/km^2)$, the land area highly suitable for development $CA(km^2)$, and the efficiency of the PV plant in converting sunlight into electricity η. This assessment method has been widely used in past studies (Charabi and Gastli, 2011; Gastli and Charabi, 2010). Based on the above parameters, the theoretical annual PV power generation potential can be calculated by the following equation as in Equation 19:

$$SGP = SR \times CA \times AF \times \eta \quad (19)$$

Where, AF denotes the actual coverable percentage of solar panels in the suitable area. In this study, η is measured data from two PV power plants in Qinghai Province: η is taken to be 23.6%; meanwhile, according to the "Report on Forest, Grassland and Sandland Utilization Zoning for PV Industry", the percentage of highly suitable theoretically coverable buildable area in Qinghai Province is 15%, AF is 15%.

2.4.3.2 Carbon emission reduction from photovoltaic power generation

Based on the total standard coal consumption given by the national standard DB21/1620-2008 (Zhao et al., 2024), CO_2 emissions are closely related to the regional fossil fuel combustion and the corresponding carbon emission factors, and their calculation follows the IPCC guidelines as in Equation 20.

$$CE = b \times SGP \times EF \quad (20)$$

where b is the standard coal consumption for power generation (g/kWh). According to the data of the National Electric Power Industry Statistical Annual Report 2021 released by China Electricity Council (China Electricity Council, 2021)., the national average coal consumption rate b for power supply is 302.5 g/kWh, and CE denotes the carbon emission (tCO_2). Is the emission factor, and EF denotes the CO_2 emission produced by burning one ton of standard coal, and its specific value is 2.54t.

3 Results

3.1 Suitability evaluation factor weighting results

3.1.1 Subjective and objective empowerment

This paper uses fuzzy analytic hierarchy process and entropy weight method to calculate subjective and objective weights, respectively. The weight results are shown in Table 3 below.

From the subjective weighting results, it can be seen that the criterion layer with the greatest impact on power generation capacity suitability is resource climate, while the one with the least impact is development cost. At the indicator layer, the factors with a significant impact on power generation capacity are land use type, total solar radiation, and sunshine duration, while those with a lesser impact include tertiary road type and distance from urban areas.

From the objective weighting results, it can be seen that primary roads, secondary roads, tertiary roads, distance from urban areas, and slope are important factors influencing suitability, with weights of 0.149 each. The information entropy values are small, indicating significant differences between samples and high information contribution. Conversely, the weights for land use type and total solar radiation are low at 0.002 and 0.005, respectively, with large entropy values and low data dispersion, thus having a minor impact on evaluation results.

3.1.2 Game theory combination weighting

Based on the results of the subjective and objective weight analysis, this study optimizes the combination of the two types of weights using game theory. By constructing a weight combination model, the objective function is to minimise the deviation between the subjective and objective weights, and the optimal combination coefficients $\alpha_1^* = 0.474$ and $\alpha_2^* = 0.526$ under the Nash equilibrium state are obtained. Based on this, the final weight determination combination formula is established as follows as in Equation 21:

$$\varpi_i = 0.474\omega_{1i} + 0.526\omega_{2i} \quad (21)$$

The calculation results for the weighting of each indicator combination are shown in Table 4.

As can be seen from the table, among the many influencing factors, primary roads, slope, and land use type are considered core indicators affecting the potential for PV power generation, significantly influencing the final assessment results; while environmental factors such as surface temperature and humidity have a relatively weaker impact.

TABLE 3 Subjective and objective weighting results table.

Indicator	Subjective weighting	Largest eigenvalue	CI	CR	Weighted subjective weighting	Information entropy value e	Objective weighting
basic geography	0.33	3.07	0.0374	0.0644	-	-	-
Resource climate	0.50				-	-	-
development costs	0.17				-	-	-
solar radiation	0.37	7.57	0.0946	0.0716	0.186	0.9991	0.0053
sunshine hours	0.22				0.110	0.9996	0.0024
Precipitation	0.11				0.056	0.9996	0.0024
Air temperature	0.12				0.062	0.9995	0.0028
Wind speed	0.06				0.033	0.9996	0.0024
Relative humidity	0.06				0.028	0.9995	0.0028
Surface temperature	0.06				0.028	0.9996	0.0024
Slope	0.24	3.01	0.0047	0.0082	0.078	0.9639	0.1493
Slope direction	0.14				0.047	0.9843	0.0876
Land use	0.62				0.204	0.9999	0.0015
Secondary roads	0.15	5.18	0.0457	0.0408	0.026	0.9580	0.1493
Tertiary roads	0.08				0.014	0.9305	0.1493
Urban locations	0.11				0.018	0.9634	0.1493
Distance from railways	0.23				0.038	0.9743	0.1437
Primary roads	0.43				0.072	0.9626	0.1493

TABLE 4 Game theory combination weighting results table.

Principles layer	Indicators layer	Weights
Resource climate	Air temperature	0.0308
	Precipitation	0.0280
	Surface temperature	0.0146
	Wind speed	0.0168
	Humidity	0.0148
	Solar radiation	0.0910
	Sunshine hours	0.0531
Development costs	Third-class road	0.0851
	Second-class road	0.0908
	First-class road	0.1128
	Railway	0.0936
	Distance from town	0.0869
Basic geography	Slope aspect	0.0685
	Slope gradient	0.1155
	Land use	0.0976

3.2 Comprehensive evaluation of the suitability of land use for the photovoltaic industry

3.2.1 Interval mapping of suitability evaluation factors

This paper combines data characteristics and follows the relevant procedures and policy documents (Ministry of Water Resources, 2024; Ministry of Land and Resources and other ministries, 2024; State Forestry Administration, 2024) to standardise and grade 15 factor layers, as shown in Table 5. In cases where the procedures do not provide clear specifications, this paper uses the quantile method to divide the grades into four levels, corresponding to four points, 3 points, 2 points, and 1 point, respectively, based on the local characteristics of Qinghai Province.

This paper categorises land use types into five categories and assigns numerical values based on relevant standards: farmland and water bodies are assigned a value of 0, forests, grasslands, and wetlands are assigned a value of 1, impervious surfaces and shrublands are assigned a value of 2, snow and ice areas are assigned a value of 3, and wastelands are assigned a value of 4. This assignment method facilitates quantitative processing and comparison of different land types in subsequent analyzes.

TABLE 5 Interval mapping of suitability evaluation factors.

Indicator layer	I	II	III	IV
Air temperature	[257,264]	[264,266]	[266,269]	[269,279]
Precipitation	[33,49]	[49,56]	[56,60]	[60,69]
Surface temperature	[0,4]	[4,6]	[6,8]	[8,10]
Wind speed	[0,6]	[6,7]	[7,9]	[9,10]
Humidity	[267,273]	[273,276]	[276,280]	[280,284]
Solar radiation	[1019.23,1380]	[1380,1650]	[1650,1820]	[1820,2480]
Sunshine hours	[532,581]	[581,601]	[601,678]	[678,813]
Tertiary road	[02,986.03]	[2,986.03,7465.07]	[7465.07,14,930.14]	[14,930.14,190,359.25]
Secondary road	[07,221.61]	[7221.61,20,633.16]	[20,633.16,44,361.30]	[44,361.30,263,072.84]
Distance from primary road	[09,299.72]	[9299.72, 29,061.64]	[29,061.64, 66,260.53]	[66,260.53, 296,428.69]
Railway	[0, 36,319.37]	[36,319.37, 97,488.84]	[97,488.84, 20,0712.31]	[20,0712.31, 487,444.19]
Distance from town	[0, 6,556.92]	[6556.92, 13,113.83]	[13,113.83, 24,042.02]	[24,042.02, 185,779.27]
Slope direction	[0, 73.61]	[73.61, 172.69]	[172.69, 259.04]	[259.04, 360.95]
Slope gradient	[0, 1.23]	[1.230, 5.21]	[5.21, 14.39]	[14.39, 78.09]

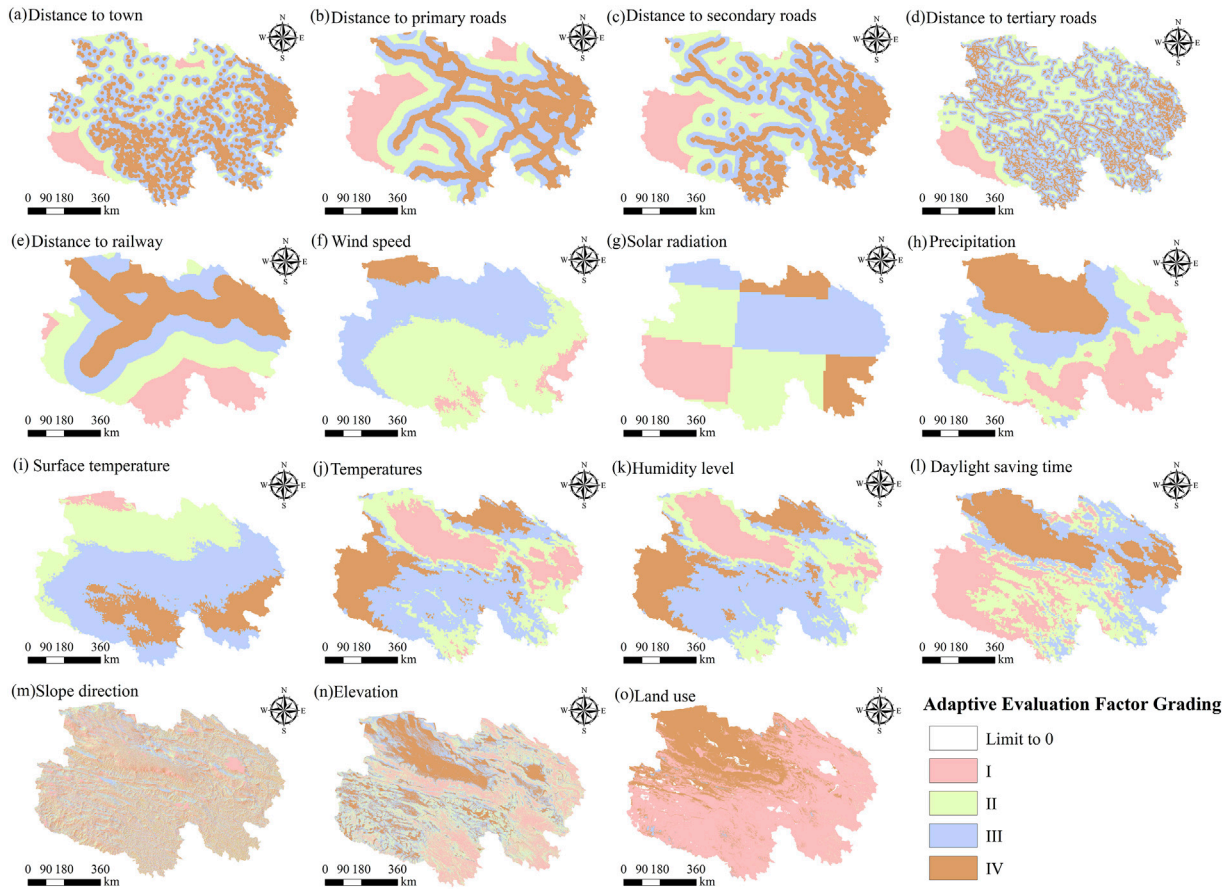

FIGURE 3
Suitability evaluation factors for PV industry development. (a) Distance to town, (b) Distance to primary roads, (c) Distance to secondary roads, (d) Distance to tertiary roads, (e) Distance to railway, (f) Air velocity, (g) Solar radiation, (h) Precipitation, (i) Surface temperature, (j) Temperatures, (k) Humidity level, (l) Daylight saving time, (m) Slope direction, (n) Elevation, (o) Land use.

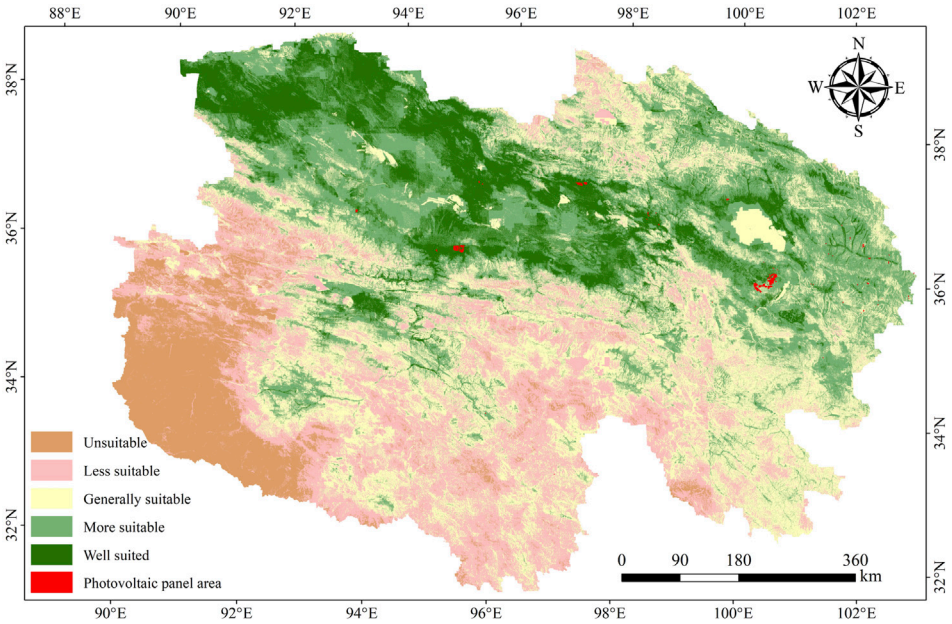

FIGURE 4
Map of suitable areas for PV industry land use.

The distribution of PV industry development suitability evaluation factors is shown in Figure 3. Areas with high ratings for factors such as distance to railways, precipitation, wind speed, sunshine duration, slope, and land use are mainly concentrated in the northwestern region. In contrast, the eastern region has relatively low ratings for all suitability factors.

3.2.2 Comprehensive suitability evaluation results and spatial distribution

Based on the comprehensive scores of various regions in Qinghai Province, the site suitability was categorized into five levels using the natural breakpoint method, as follows: unsuitable (0.33–0.51), moderately unsuitable (0.51–0.58), generally suitable (0.58–0.64), moderately suitable (0.64–0.71), and highly suitable (0.71–0.88). The proportions of each category relative to the total area of the province are 8.46%, 22.06%, 30.64%, 26.28%, and 12.56%, respectively. The results indicate that most regions have moderate or higher suitability, demonstrating good potential for PV development.

The PV panel area shown in Figure 4 represents the current distribution of PV industry land use in Qinghai Province as of 2022. Approximately 69.48% of Qinghai Province's total area has been identified as suitable for PV development. The land suitability in Qinghai Province exhibits a distinct north-south gradient. Due to the impact of sandstorms and air pollution, solar resources in the southern regions are relatively scarce. Additionally, since most southern regions have high elevations, the construction and maintenance costs for PV projects are relatively expensive. Therefore, the most suitable and moderately suitable areas are primarily concentrated in the Qaidam Basin and around Qinghai Lake, while the unsuitable areas are mainly located in the Haixi Mongolian and Tibetan Autonomous Prefecture (southwest).

In terms of spatial distribution, PV power stations are mainly located in the Haibei Mongolian and Tibetan Autonomous Prefecture (southeast) and the Hainan Tibetan Autonomous Prefecture (southeast). These areas largely overlap with regions of high suitability, and they are characterized by abundant solar resources, convenient transportation, and relatively low construction costs.

3.3 Analysis of the development potential of land for the photovoltaic industry

3.3.1 Restricted areas

The siting of Photovoltaic power stations must meet nature conservation requirements, while also balancing construction costs and economic benefits. Based on existing literature, the implementation rules of Qinghai Province's 'Measures for the Administration of Forest and Wildlife Nature Reserves,' and the General Administration of Quality Supervision, Inspection and Quarantine, this paper identifies four key limiting factors (see Figure 5).

Nature reserves are divided into core areas, buffer zones, and experimental zones. Entry into core areas is prohibited, buffer zones are used for scientific research and monitoring, and experimental zones can be used for scientific research, teaching, and species breeding activities. Therefore, this study uses core areas, protected areas, and buffer zones as the main constraints.

With regard to land use types, this paper combines relevant literature (Ministry of Natural Resources, 2024) to impose corresponding restrictions on four types of land: farmland, water bodies, impervious surfaces, and permanent snow cover.

In addition, steep slopes will significantly increase costs related to transportation, installation, and cleaning. Therefore, areas with

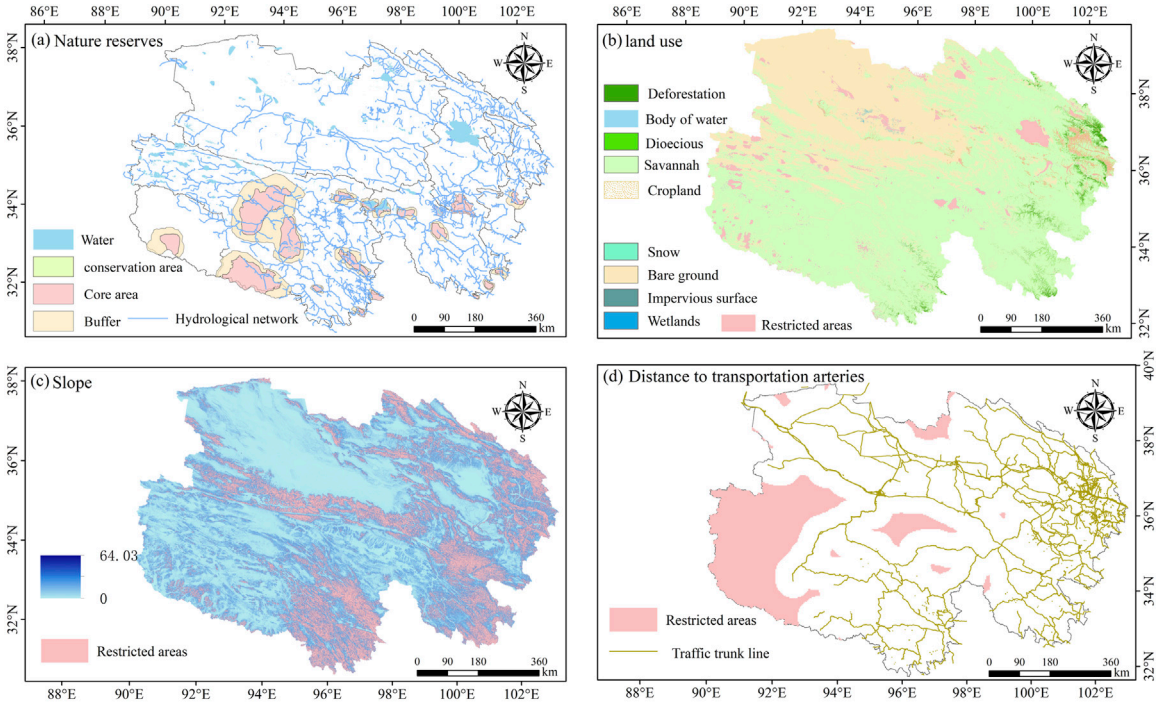

FIGURE 5
Restricted area. **(a)** Nature reserves, **(b)** land use, **(c)** Slope, **(d)** Distance to transportation arteries.

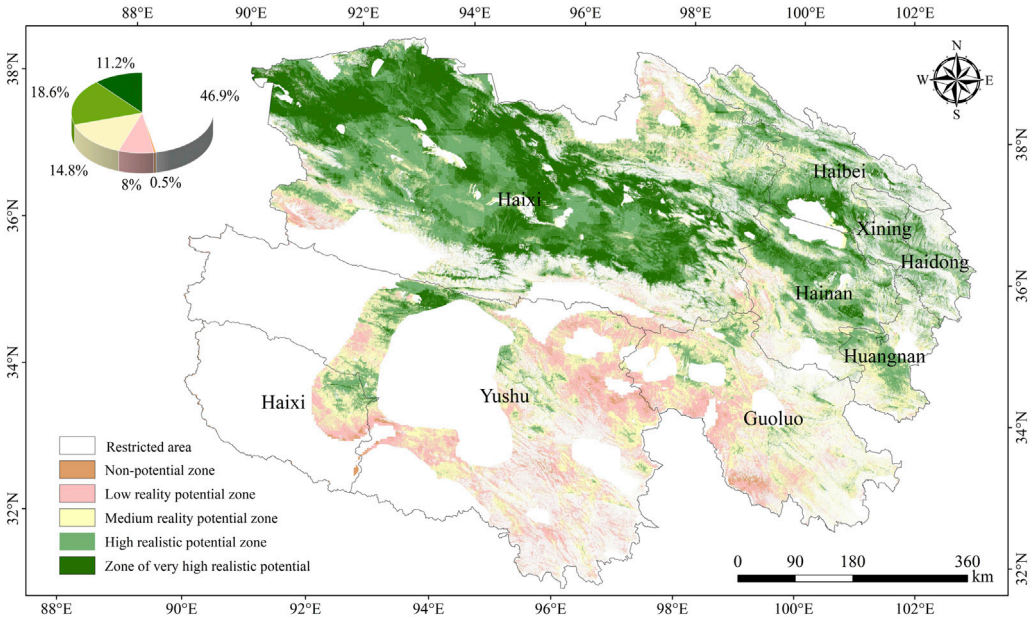

FIGURE 6
Regional distribution of areas with realizable potential.

slopes less than 15% are considered suitable for PV power station construction (Cheng et al., 2022). Areas with slopes exceeding 15% are defined as restricted areas.

Given that the distance from major transportation routes has a direct impact on construction convenience, areas located more than 50 km from major transportation routes face numerous challenges in terms of equipment procurement and power transmission. Therefore, this factor has also become an important limiting condition in regional selection (Tripathy et al., 2018).

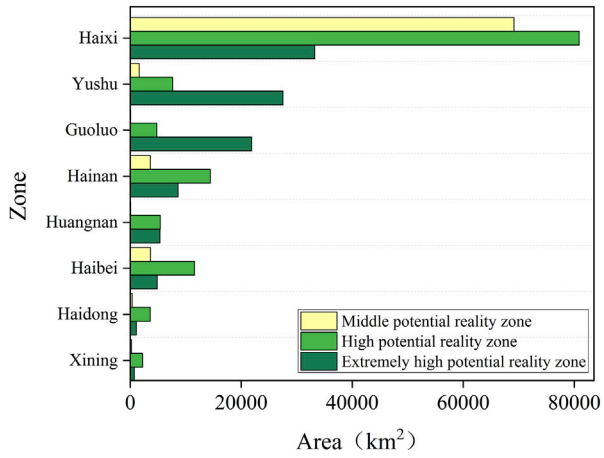

FIGURE 7
Potential area for PV power generation in various regions.

In addition to the aforementioned restricted areas, corresponding restrictions should also be set for developed areas to more accurately assess PV potential areas. Specifically, PV panels should not be installed within nature reserves and their 2-km buffer zones; farmland, water bodies, impermeable surfaces, and areas with permanent snow cover are all considered restricted areas; areas with slopes exceeding 15% are also excluded; additionally, areas more than 50 km from major and minor roads are designated as unsuitable for Photovoltaic panel installation.

3.3.2 Spatial distribution of areas with realizable potential

To enhance the practical significance of the results of this study, in addition to calculating the suitability scores for various regions in Qinghai Province, we further introduced restricted areas to identify regions with realizable PV development potential. Regions with realizable PV land development potential refer to areas that have not yet been used for PV construction and that have development potential after meeting specific conditions. Based on the suitability zoning, this paper added the above restrictions to determine the regions with realizable PV land development potential. The distribution of each potential region is shown in Figure 6.

The total area of PV construction land with realizable development potential in the region is 366,800 km^2, accounting for 52.61% of Qinghai Province's total area; the total area of restricted zones is 327,100 km^2, accounting for 46.91% of the total area. Based on suitability zoning, this study categorises the potential areas into five types: extremely high, high, medium, low, and non-potential, accounting for 11.2%, 18.6%, 14.8%, 8%, and 0.5% of the total area, respectively. Among these, high-potential areas are primarily concentrated in the northern part of Qinghai Province, particularly in the Haixi Mongolian and Tibetan Autonomous Prefecture, covering nearly the entire Qaidam Basin.

Non-potential areas and low-potential areas are mainly distributed in southern Qinghai Province. These areas are characterized by complex terrain, sparse population, and limitations in infrastructure such as transportation, which are unfavourable for the construction and development of PV power stations. Therefore, considering these factors, southern Qinghai Province does not have the advantages for large-scale PV development.

Based on the geographical information of Qinghai Province, the spatial distribution of potential areas is characterized by 'three belts and two zones'. The three belts are: the high-potential zone comprising the Qaidam Basin and the area south of the Qilian Mountains-Datong Mountains-Laojishan Mountains; the medium-potential zone comprising the area south of the Shule South Mountains-Akon Mountains-Qinghai South Mountains-Eola Mountains-Animaqin Mountains; and the low-potential zone comprising the area formed by the Daji River-Bayankada Mountains-Chumar River-Tongtian River and the Zagsuinao-Tongtian River-Baicha -Zanarigen. The formation of the low-potential zone may be related to factors such as lower total solar radiation, steeper terrain slopes, and higher construction costs in the region. The two main areas are: the vicinity of the Qaidam Basin and the vicinity of Qinghai Lake, where extremely high-potential zones are distributed, with high annual average radiation levels and favourable development conditions.

As can be seen from Figure 7, Haixi Mongolian and Tibetan Autonomous Prefecture (northwest) and Yushu Tibetan Autonomous Prefecture demonstrate significant potential for the PV industry, primarily due to their flat terrain, high solar radiation levels, prolonged sunshine hours, and extensive undeveloped land. In particular, the eastern part of Yushu has relatively dense transportation infrastructure, which helps reduce construction costs. However, the southwestern part of Haixi has weaker solar radiation and steeper slopes, resulting in lower PV development potential. Currently, the PV land development in both regions has not fully tapped its potential. In the future, priority should be given to developing unused land such as deserts, and PV power stations should be integrated with the 'Three Norths' Shelterbelt Project to promote clean energy supply and ecological conservation.

Golok Tibetan Autonomous Prefecture, Hainan Tibetan Autonomous Prefecture, and Huangnan Tibetan Autonomous Prefecture offer significant potential for the development of PV power generation due to their unique geographical and climatic conditions. Golok Prefecture is located in the southeastern part of Qinghai Province, primarily characterized by high mountain gorges and glacial permafrost landscapes; Hainan Prefecture is situated in the northeastern part, near Qinghai Lake, with terrain features dominated by highland mountains and lakeside plains; Huangnan Prefecture is located in the southeastern part, adjacent to Golok and Hainan Prefectures, with its river valley terraces serving as an important hub for power transmission. The natural environmental characteristics of these regions make the border areas between the three prefectures rich in PV power generation potential, particularly in terms of spatial layout for PV energy development, where complementary advantages can be formed.

3.4 Coupling analysis of photovoltaic potential and energy demand

Bivariate local Moran's I is an important method for spatial data analysis, mainly used to analyze the correlation between two

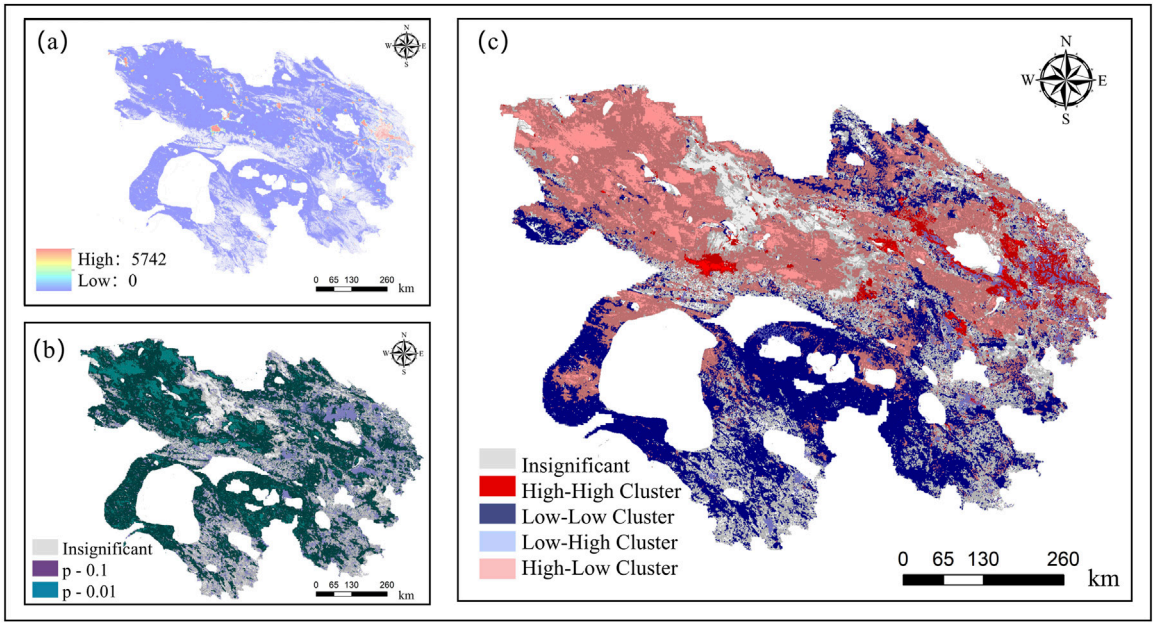

FIGURE 8
Correlation between PV potential and electricity consumption. **(a)** Spatial distribution of electricity consumption; **(b)** significance level; **(c)** clustering.

variables in space. It assesses the similarity between neighbouring areas by calculating the local spatial autocorrelation of variables at a given location.

Night-time lighting can reflect local electricity demand in the region (Wati and Meukam, 2024; Wang et al., 2024a; Liu et al., 2024). This paper used Geoda software to perform a binary local Moran's I analysis to assess PV potential and electricity consumption (Figure 8). The results were divided into the following clusters: high potential-high demand, low potential-low demand, low potential-high demand, and high potential-low demand clusters.

The results show that Moran's I p-value is 0.001 and Z-value is 114.28. This indicates that there is significant spatial autocorrelation between PV potential and electricity consumption.

High-potential, high-demand areas are mainly distributed in the southern part of the Qaidam Basin, the northern part of the Qinghai Mountains, the northwestern part of the Taka Salt Lake, and Xining City and its surrounding areas. These areas show active economic activity and convenient transportation, which is conducive to the construction of PV power stations. Low-potential, low-demand areas are mainly distributed in the southern or central part of the Qinghai-Tibet Plateau, parts of the Bayan Kara Mountains and the southern Shule Mountains. These areas are at high altitudes with little economic activity. Although there is potential for PV power generation, the infrastructure is relatively weak. Low-potential, high-demand areas are mainly distributed in cities and industrial zones with concentrated economic activity in Qinghai Province, such as Xining and its surrounding areas. These areas have high energy demand, but due to geographical conditions (such as mountainous or desertified areas), the potential for PV resource development is low. In contrast, high-potential, low-demand areas are mainly distributed in the Qaidam Basin, parts of the plateau, and mountainous regions. These areas have abundant PV resources and are suitable for large-scale PV power station construction, but due to their sparse population and limited economic activity, energy demand is relatively low.

Therefore, for high-potential, high-demand areas, their locational advantages should be fully leveraged to promote the coordinated development of PV power generation bases and industrial parks, thereby achieving efficient development of solar energy resources while promoting the clustering of energy-intensive industries. For areas with similar development conditions but limited local consumption capacity, it is more appropriate to develop them as clean energy export bases, utilising ultra-high voltage transmission channels to achieve intensive use of land resources and cross-regional energy coordination and development.

3.5 Comprehensive analysis of carbon emission reduction benefits

The progress of PV construction in Qinghai Province's highly suitable areas can be divided into four different scenarios: 25%, 50%, 75% and 100% construction progress. The calculation results are shown in Table 6.

The results indicate that Qinghai Province has enormous potential for PV power generation, with an annual power generation capacity of approximately 2.043×10^7 GWh. The construction of these PV power plants will significantly reduce fuel consumption and provide significant environmental benefits in terms of CO_2 emissions reduction. Even if only 25% of the construction is completed, the potential power generation capacity will be sufficient to meet Qinghai Province's annual power demand.

This paper employs four regression algorithms—linear regression, Lasso regression, elastic net regression, and Ridge regression—to predict PV power generation from 2019 to

TABLE 6 Power generation potential and emission reduction effects.

Construction progress	Highly suitable land area (km²)	Theoretical potential (GWh)	Carbon emissions (tCO2)
25%	77,920.32	5,106,753	3,923,773,642.93
50%	155,840.65	10,213,506	7,847,547,285.87
75%	233,760.97	15,320,259	11,771,320,928.80
100%	311,681.29	20,427,012	15,695,094,571.73

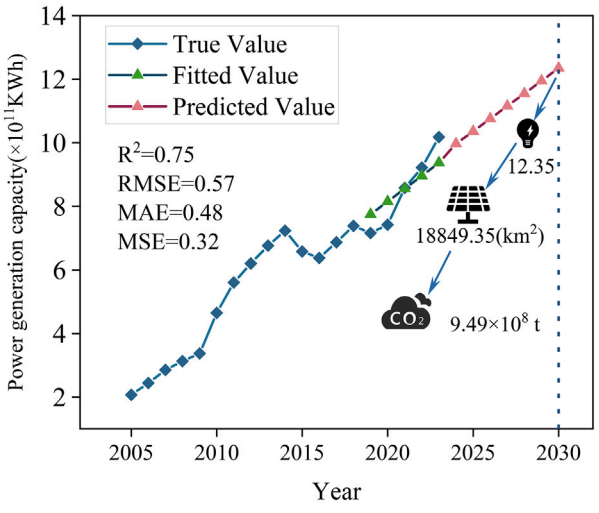

FIGURE 9
Visualisation of carbon emission reduction benefits.

2023 and evaluates the performance of the models. The results show that Ridge regression performs best across all metrics, with an R^2 value of 0.75, mean squared error (MSE) of 0.32, root mean squared error (RMSE) of 0.57, and mean absolute error (MAE) of 0.48. In contrast, Lasso regression achieved an R^2 value of 0.71, demonstrating strong predictive capability, while linear regression had an R^2 value of only 0.38, indicating relatively weaker predictive performance. Overall, regularized regression models demonstrated superior performance in predicting PV power generation.

Through comparison, the ridge regression model outperformed other models in predicting Qinghai's PV power generation from 2019 to 2023, demonstrating good fit and high prediction accuracy. The R^2 value was 0.75, indicating that the model could explain 75% of the changes in the target variable. Additionally, the low RMSE (0.57), MAE (0.48), and MSE (0.32) values indicated that the model's prediction results deviated minimally from the actual values. Therefore, this paper selects the ridge regression model to predict Qinghai Province's electricity generation for the period 2025–2030.

As shown in the prediction results in Figure 9, Qinghai Province's electricity consumption in 2030 is projected to be 1.235×10^{12} KWh. To meet Qinghai Province's future electricity demand, the province should theoretically construct PV panels with a total area of 18,849.35 km². Based on the electricity generation per square kilometer, the electricity generated by these PV panels would reduce carbon dioxide emissions by 9.49×10^8 tonnes compared to traditional power generation methods, thereby significantly mitigating the impact of the greenhouse effect.

4 Discussion

This study constructs a systematic evaluation system for the suitability of PV development based on multidimensional factors such as geography, climate, transportation, land use, and energy demand in Qinghai Province, and further identifies achievable areas of PV potential as well as carbon emission reduction benefits. The core findings of the study results are discussed below, and their practical significance, innovativeness and limitations are analyzed.

In this paper, in terms of the construction of the indicator system, an evaluation indicator system containing 3 guideline layers and 15 indicator layers is constructed based on the existing literature. Compared with previous studies (Wati and Meukam, 2024; Wang et al., 2024; Liu et al., 2024) that focused only on the single dimension of resource endowment or environmental factors, this paper is more comprehensive and applicable in the selection of indicators. By introducing the combined assignment method of improved FAHP and improved entropy weight method, and using game theory for optimization and integration, the differences between subjective judgment and objective data are better coordinated, and the scientificity and reliability of weight determination are effectively improved. According to the above method, the evaluation system of PV power generation siting suitability is established by combining TOPSIS, and the suitability analysis is carried out.

In the spatial suitability analysis, the results show that 69.48% of the area of Qinghai Province is suitable for development, which verifies the geographical advantage of Qinghai as a national clean energy base. Meanwhile, the suitability shows an obvious spatial gradient of "high in the west and low in the east" and "poor in the south and rich in the north", a spatial pattern that is closely related to natural factors such as topography, solar radiation, slope, etc., which further confirms the reasonableness of the selected evaluation index system. Comparison with the distribution of existing PV sites shows that the current PV development is concentrated in high suitability zones, which empirically strengthens the application value of the evaluation system of this study.

In order to improve the practical application value of the research results, this paper identifies the developable areas in Qinghai Province based on the assessment of PV suitability zones, combined with the requirements of territorial spatial planning and policies, and the comprehensive consideration of factors such as nature reserves, land use types, topographic data, the current status of PV, and the suitability of transportation, etc. On

the basis of which, combined with the suitability assessment, it arrives at the achievable PV potential zones. Research shows that the total area of developable PV construction land in the region is 366,800 km^2, accounting for 52.61% of the total area of Qinghai Province, and presenting the spatial distribution characteristics of "three belts and two slices". Among them, Qaidam Basin and Qinghai Lake have outstanding development advantages, and it is recommended to prioritize the layout of light storage integration demonstration bases. This conclusion provides a spatial decision-making basis for the government's land control and resource integration.

To further assess the local correlation patterns between photovoltaic potential and electricity consumption, this study employs the binary local Moran's I index to analyze the coupling relationship between photovoltaic potential and electricity demand. The results reveal significant spatial heterogeneity and mismatch between the two. Among these, "high-potential-low-demand" regions are suitable as planning priorities, with the aim of establishing clean energy export bases to maximize resource output. "High potential-high demand" regions possess advantages for developing distributed photovoltaic storage and power synergy systems, which can help achieve a match between local electricity consumption and load response. This analysis provides a theoretical basis for the spatial optimization of regional energy systems, contributing to improved utilization efficiency of photovoltaic power generation and overall stability of power system operations.

In order to contribute to the development of clean energy in Qinghai Province, this paper systematically quantifies the Photovoltaic power generation potential and carbon emission reduction benefits in the region, and compares and predicts the province's electricity demand in 2030 using a variety of models, including ridge regression. The results show that the average annual CO_2 emission reduction potential of Qinghai Province can reach 1,570 million tons under the 100% high suitability zone development scenario. The prediction results show that by 2030, the total annual electricity consumption in Qinghai Province will reach 1.235×10^{12} kWh. In order to achieve a balance between energy supply and demand, about 18,849.35 km^2 of Photovoltaic power generation facilities will need to be constructed, which is expected to reduce CO_2 emissions by about 9.48×10^8 t. The results of this research can provide data support for the energy authorities to scientifically prepare the scale of new installations, and also provide a quantitative basis for the regionalized design of the carbon trading mechanism and carbon subsidy policy at the national level.

This study identified developable areas based on geographical, environmental, and certain policy factors. However, some areas may not be developable due to actual policy restrictions. For example, in China, ecological protection red line areas (Wang, et al., 2024a) and permanent basic farmland (Cheng et al., 2017) are legally prohibited from development. Therefore, when conducting development, it is necessary to combine national and local land use planning and relevant policy requirements to improve practicality and feasibility.

This study has achieved more systematic results in terms of integrating multi-dimensional indicators, identifying regional development, and assessing the benefits of carbon emission reductions, it still has some limitations. For example, this study is based on static data and cannot dynamically capture future changes in land policies and evolving market trends. Additionally, due to data limitations, the model does not incorporate certain socioeconomic factors (such as policy support and land costs). In the future, the SD-GIS coupling method proposed by Pakere et al. (2022) (Pakere et al., 2022) could be adopted to conduct annual iterations of subsidies, loads, and land policies. Additionally, the "annual recalculation" method proposed by Sun et al. (2025) could be referenced to dynamically update the weights and suitability scores of each grid cell at each time step. This method can real-time reflect the impact of factors such as ecological red line adjustments, subsidy changes, and rising land costs on the layout of photovoltaic site selection, thereby enhancing the forward-looking nature and decision-making value of the results.

5 Conclusion

It is crucial to analyze regional suitability and potential in siting PV power generation construction. In this paper, the regional suitability, power generation potential and emission reduction effect of Qinghai Province are comprehensively assessed by collecting data from multiple sources and processing and analyzing them using software. The main conclusions are as follows:

Based on multi-source data and combined with PV land use control regulations, this paper constructs a PV land use suitability evaluation system for Qinghai Province that contains 3 guideline layers and 15 indicators, and adopts the game theory combination assignment method to determine the weights of the indicators, which takes into account the subjective and objective factors to enhance the interpretability of the results. The results show that slope, secondary road and land use type are the main influencing factors.

The suitability of the whole region of Qinghai Province shows significant spatial heterogeneity, in which the area of suitable development areas is 4.85×10^5 km^2, accounting for 69.48% of the total area. Geographically, these suitable areas are mainly concentrated in the Qaidam Basin and around Qinghai Lake. Spatially, these areas show the gradient distribution characteristic of "high in the west and low in the east". In addition, the distribution of land for the PV industry in Qinghai Province is mainly concentrated in areas with higher suitability.

The development potential of PV industrial land in Qinghai Province is huge, with remarkable development space. The total area of potential areas for development is 366,800 km^2, accounting for 52.61% of the total area of Qinghai Province. The spatial distribution of these potential areas is characterized by 'three belts and two patches', with significant differences in the development potential of Photovoltaic industry land use in different areas. The areas with higher potentials are mainly distributed in Hainan Mongolian and Tibetan Autonomous Prefecture, Haibei Tibetan Autonomous Prefecture and the surrounding areas of Hainan Tibetan Autonomous Prefecture, which have higher development potentials and are the key areas for the development of PV industrial land. In addition, the results of Moran's I show that

there is a significant coupling relationship between PV potential and electricity consumption in Qinghai Province.

When the PV construction process in highly suitable areas of Qinghai Province reaches 25%, its potential power generation capacity meets the annual power demand of the province. With the full development of PV power plants, the theoretical potential of annual PV power generation in Qinghai Province can reach 2.043×10^7 GWh, which is equivalent to about 6.18×10^9t of coal. At the same time, the promotion of PV power generation is expected to significantly reduce carbon dioxide emissions, which can be reduced by $1.57 \times 10^{10}tCO_2$ annually. According to the prediction of power consumption in Qinghai Province in 2030 (1.235×10^{12} KWh), if 18,849.35 km^2 of PV power plant is constructed, it will be sufficient to meet the province's power demand. The area of this PV power plant is about 6% of the realizable potential area and is expected to reduce about 9.49×10^8tCO_2 emissions.

Data availability statement

The datasets presented in this study can be found in online repositories. The names of the repository/repositories and accession number(s) can be found below: (https://doi.org/10.5281/zenodo.15660931), (https://doi.org/10.5281/zenodo.15660905).

Author contributions

JH: Methodology, Writing – original draft, Software, Data curation, Writing – review and editing. SW: Writing – original draft, Investigation, Data curation, Writing – review and editing, Visualization, Validation. BZ: Investigation, Software, Writing – review and editing, Visualization, Writing – original draft, Methodology. QZ: Funding acquisition, Project administration, Supervision, Writing – review and editing, Methodology, Writing – original draft.

Funding

The author(s) declare that financial support was received for the research and/or publication of this article. This research was funded by the Key Research and Development Project of the Sichuan Provincial Department of Science and Technology (Grant No. 2024YFFK0191) and the Chunhui Programme of the Ministry of Education of China (Grant No. 202201245).

Conflict of interest

The authors declare that the research was conducted in the absence of any commercial or financial relationships that could be construed as a potential conflict of interest.

Generative AI statement

The author(s) declare that no Generative AI was used in the creation of this manuscript.

Any alternative text (alt text) provided alongside figures in this article has been generated by Frontiers with the support of artificial intelligence and reasonable efforts have been made to ensure accuracy, including review by the authors wherever possible. If you identify any issues, please contact us.

Publisher's note

References

Al-Abadi, A. M., Handhal, A. M., Abdulhasan, M. A., Ali, W. L., Hassan, J. J., and Al Aboodi, A. H. (2025). Optimal siting of large photovoltaic solar farms at basrah governorate, southern Iraq using hybrid GIS-based Entropy-TOPSIS and AHP-TOPSIS models. *Renew. Energy* 241, 122308. doi:10.1016/j.renene.2024.122308

Amrani, S. E., Merrouni, A. A., Touili, S., El Gharad, A., and Mezrhab, A. (2023). A multi-scenario site suitability analysis to assess the installation of large-scale photovoltaic-hydrogen production units. Case study: eastern Morocco. *Energy Convers. Manag.* 295, 117615. doi:10.1016/j.enconman.2023.117615

Antonanzas, J., Osorio, N., Escribano, A., Martínez-de-Pisón, F. J., Antonanzas-Torres, F., Van Deventer, W., et al. (2018). Forecasting of photovoltaic power generation and model optimization: a review. *Renew. Sustain. Energy Rev.* 81, 912–928. doi:10.1016/j.rser.2017.08.017

Charabi, Y., and Gastli, A. (2011). PV site suitability analysis using GIS-based spatial fuzzy multi-criteria evaluation. *Renew. Energy* 36 (9), 2554–2561. doi:10.1016/j.renene.2010.10.037

Chen, X., Zhou, C., Tian, Z., Liu, J., Wang, Y., Huang, H., et al. (2023). Different photovoltaic power potential variations in east and west China. *Appl. Energy* 351, 121846. doi:10.1016/j.apenergy.2023.121846

Cheng, Q., Jiang, P., Cai, L., Shan, J., Zhang, Y., Wang, L., et al. (2017). Delineation of a permanent basic farmland protection area around a city centre: case study of changzhou city, China. *Land Use Policy* 60, 73–89. doi:10.1016/j.landusepol.2016.10.014

Cheng, C., Gutierrez, N. P., Blakers, A., Elliston, B., Lu, B., and Stocks, M. (2022). GIS-based solar and wind resource assessment and least-cost 100 % renewable electricity modelling for Bolivia. *Energy sustain. Dev.* 69, 134–149. doi:10.1016/j.esd.2022.06.008

China Electricity Council (2021). Annual development report of China's electric power industry, 2021 [M/EB/OL]; China building materials industry press.

de Luis-Ruiz, J. M., Salas-Menocal, B. R., Pereda-García, R., Pérez-Álvarez, R., Sedano-Cibrián, J., and Ruiz-Fernández, C. (2024). Optimal location of solar photovoltaic plants using geographic information systems and multi-criteria analysis. *Sustainability* 16, 2895. doi:10.3390/su16072895

Elboshy, B., Alwetaishi, M., Aly, R. M. H., and Zalhaf, A. S. (2022). A suitability mapping for the PV solar farms in Egypt based on GIS-AHP to optimize multi-criteria feasibility. *Ain Shams Eng. J.* 13, 101618. doi:10.1016/j.asej.2021.10.013

Fang, H., Li, J., and Song, W. (2018). Sustainable site selection for photovoltaic power plant: an integrated approach based on prospect theory. *Energy Convers. Manag.* 174, 755–768. doi:10.1016/j.enconman.2018.08.092

Feng, F., and Wang, K. (2020). High-resolution (10 km) surface solar radiation dataset (1983–2017) based on integrated sunshine duration across China. *Natl. Tibet. Plateau Data Cent.*

Feng, X., Zhang, Z., Chen, Q., Guo, Z., Zhang, H., Wang, M., et al. (2025). Integrating remote sensing, GIS, and multi-criteria decision making for assessing PV potential in mountainous regions. *Renew. Energy* 241, 122340. doi:10.1016/j.renene.2025.122340

GaryBikini (2023). ChinaAdminDivisonSHP v23.01.04. *Zenodo*. doi:10.5281/zenodo.

Gastli, A., and Charabi, Y. (2010). Solar electricity prospects in Oman using GIS-based solar radiation maps. *Renew. Sustain. Energy Rev.* 14 (2), 790–797. doi:10.1016/j.rser.2009.08.018

Gholami, A., Ameri, M., Zandi, M., Goudarzi, N., Reisi, M., and Pierfederici, S. (2020). Photovoltaic potential assessment and dust impacts on photovoltaic systems in Iran: review paper. *IEEE J. Photovolt.* 10, 824–837. doi:10.1109/JPHOTOV.2020.2978851

Ghosh, S., Kumar, A., Ganguly, D., Singh, R., Sharma, A., and Tiwari, A. (2023). India's photovoltaic potential amidst air pollution and land constraints. *iScience* 26, 107856. doi:10.1016/j.isci.2023.107856

Jerez, S., Tobin, I., Vautard, R., Montávez, J. P., De La Torre, L., López-Romero, J. M., et al. (2015). The impact of climate change on photovoltaic power generation in Europe. *Nat. Commun.* 6, 10014. doi:10.1038/ncomms10014

Li, J., Chen, S., Wu, Y., Zhang, L., Wang, T., Liu, H., et al. (2021). How to make better use of intermittent and variable energy? A review of wind and photovoltaic power consumption in China. *Renew. Sustain. Energy Rev.* 137, 110626. doi:10.1016/j.rser.2020.110626

Liu, S., Song, Z., Zhang, Y., Guo, D., Sun, Y., Zeng, T., et al. (2023). Risk assessment of deep excavation construction based on combined weighting and nonlinear FAHP. *Front. Earth Sci.* 11, 1204721. doi:10.3389/feart.2023.1204721

Liu, Y., Mu, Z., Dong, W., Huang, Q., Chai, F., and Fan, J. (2024). Establishment of an evaluation indicator system and evaluation criteria for the weihe river ecological watersheds. *Front. Earth Sci.* 11, 1204721. doi:10.3390/w16172393

Lü, X., Li, X., Wei, H., Wu, J., Dang, D., and Zhang, C. (2024). Spatial distribution dataset of solar panels in China (2000–2022). *Natl. Tibet. Plateau Data Cent*. doi:10.11888/RemoteSen.tpdc.301546

Luan, C., Liu, R., and Peng, S. (2021). Land-use suitability assessment for urban development using a GIS-based soft computing approach: a case study of ili valley, China. *Ecol. Indic.* 123, 107333. doi:10.1016/j.ecolind.2020.107333

Mahmud, K., Azam, S., Karim, A., Khan, R., Saha, T., and Mathur, D. (2021). Machine learning based PV power generation forecasting in alice springs. *IEEE Access* 9, 46117–46128. doi:10.1109/ACCESS.2021.3066494

Ministry of Land and Resources and other ministries (2024). Opinions on supporting the development of new industries and new business models to promote mass entrepreneurship and innovation [EB/OL]. Available online at: https://www.mlr.gov.cn/(accessed on July 2, 2024).

Ministry of Natural Resources (2024). Notice on supporting the development of the photovoltaic industry and regulating land use management. Available online at: https://www.mnr.gov.cn/(accessed on July 2, 2024).

Ministry of Water Resources (2024). Guiding opinions on strengthening the spatial management and control of river and lake shorelines. Available online at: https://www.mwr.gov.cn/(accessed on July 2, 2024).

Mitchell, D., Allen, M. R., Hall, J. W., Muller, B., Rajamani, L., and Le Quéré, C. (2018). The myriad challenges of the paris agreement. *Philos. Trans. R. Soc. A* 376, 20180066. doi:10.1098/rsta.2018.0066

National Energy Administration (2014). Notice on further implementing policies related to distributed photovoltaic power generation. Available online at: https://www.nea.gov.cn/.

National Energy Administration (2025). National energy administration released power industry statistics for January–February 2025 [EB/OL]. Available online at: https://www.nea.gov.cn/(accessed on April 5, 2025).

O'Shaughnessy, E., Cruce, J. R., and Xu, K. (2020). Too much of a good thing? Global trends in the curtailment of solar photovoltaic. *Sol. Energy* 208, 1068–1077. doi:10.1016/j.solener.2020.08.075

OpenStreetMap contributors (2025). OpenStreetMap [DB/OL]. Available online at: https://www.openstreetmap.org/(accessed on April 6, 2025).

Pakere, I., Kacare, M., Grāvelsiņš, A., Freimanis, R., and Blumberga, A. (2022). Spatial analyses of smart energy system implementation through system dynamics and GIS modelling: wind power case study in Latvia. *Smart Energy* 7, 100081. doi:10.1016/j.segy.2022.100081

Qinghai Provincial People's Government (2025). Geography and natural conditions [EB/OL]. Available online at: https://www.qinghai.gov.cn/(accessed on April 5, 2025).

Sahu, B. K. (2015). A study on global solar PV energy developments and policies with special focus on the top ten solar PV power producing countries. *Renew. Sustain. Energy Rev.* 43, 621–634. doi:10.1016/j.rser.2014.11.058

Sharadga, H., Hajimirza, S., and Balog, R. S. (2020). Time series forecasting of solar power generation for large-scale photovoltaic plants. *Renew. Energy* 150, 797–807. doi:10.1016/j.renene.2019.12.131

Song, Z., Cao, S., and Yang, H. (2023). Assessment of solar radiation resource and photovoltaic power potential across China based on optimized interpretable machine learning model and GIS-based approaches. *Appl. Energy* 339, 121005. doi:10.1016/j.apenergy.2023.121005

State Forestry Administration (2024). Notice on issues related to the use of forest land for photovoltaic power station construction (Doc. No. [2015] 153). Available online at: https://www.forestry.gov.cn/(accessed on July 2, 2024).

Suehrcke, H., Bowden, R. S., and Hollands, K. G. T. (2013). Relationship between sunshine duration and solar radiation. *Sol. Energy* 92, 160–171. doi:10.1016/j.solener.2013.02.026

Sui, M., and Wei, Y. (2000). Discussion and improvement of the weight determination method in Fuzzy AHP. *J. Shanxi Univ. Nat. Sci. Ed.* (3), 218–220. doi:10.13451/j.cnki.shanxi.univ(nat.sci.).2000.03.008

Sun, Y., Li, Y., Wang, R., and Ma, R. (2025). Dynamic geospatial modeling of solar energy expansion potential in China: implications for national-level optimization of solar photovoltaic plant layouts. *Energy* 333, 137433. doi:10.1016/j.energy.2025.137433

Tan, H., Guo, Z., Chen, Y., Zhang, H., Song, C., Jiang, M., et al. (2025). PV potential analysis through deep learning and remote sensing-based urban land classification. *Appl. Energy* 387, 125616. doi:10.1016/j.apenergy.2025.125616

Tong, H., Lv, Z., Jiang, J., Zhang, Y., Wang, X., Liu, M., et al. (2025). Analysis of regional photovoltaic power generation suitability in China using multi-source data. *Front. Earth Sci.* 12, 1528134. doi:10.3389/feart.2024.1528134

Tripathy, B. R., Sajjad, H., Elvidge, C. D., Kumar, P., Pandey, A. C., Rani, M., et al. (2018). Modeling of electric demand for sustainable energy and management in India using spatio-temporal DMSP-OLS night-time data. *Environ. Manag.* 61, 615–623. doi:10.1007/s00267-017-0978-1

Wang, D., Wang, H., Qu, M., Zhang, J., Liu, X., Zhao, Y., et al. (2023). Suitability evaluation and potential estimation of photovoltaic power generation and carbon emission reduction in the Qinghai–Tibet Plateau. *Environ. Monit. Assess.* 195, 887. doi:10.1007/s10661-023-11439-8

Wang, J., Zhang, Y., Liu, M., Chen, F., Zhao, Q., Du, Z., et al. (2024a). Mapping national-scale photovoltaic power stations using a novel enhanced photovoltaic index and evaluating carbon reduction benefits. *Energy Convers. Manag.* 318, 118894. doi:10.1016/j.enconman.2024.118894

Wang, L., Zheng, H., Chen, Y., and Huang, B. (2024b). Ecological redline policy strengthens sustainable development goals through the strict protection of multiple ecosystem services. *Glob. Ecol. Conserv.* 56, e03306. doi:10.1016/j.gecco.2024.e03306

Wati, E., and Meukam, P. (2024). Impact of the climate change on the site suitability for solar farms: case study of Cameroon. *Renew. Energy* 225, 120310. doi:10.1016/j.renene.2024.120310

Wu, J., Xiao, J., Hou, J., Zhang, L., Liu, Y., and Chen, Q. (2023). Development potential assessment for wind and photovoltaic power energy resources in the main desert–gobi–wilderness areas of China. *Energies* 16, 4559. doi:10.3390/en16124559

Xu, Y., Wang, M., Xu, Y., Li, X., Wu, Y., and Chi, F. (2023). Evaluation system creation and application of "zero-pollution village" based on combined FAHP-TOPSIS method: a case study of Zhejiang Province. *Sustainability* 15, 12367. doi:10.3390/su151612367

Yang, J., and Huang, X. (2023). The 30 m annual land cover dataset and its dynamics in China from 1990 to 2019. *Earth Syst. Sci. Data* 13 (1), 3907–3925. doi:10.5194/essd-13-3907-2021

Yang, Q., Huang, T., Wang, S., Liu, X., Zhang, Y., Li, J., et al. (2019). A GIS-based high spatial resolution assessment of large-scale PV generation potential in China. *Appl. Energy* 247, 254–269. doi:10.1016/j.apenergy.2019.04.005

Yuan, J. H., Sun, S. Z., Guo, X. L., Liu, Y., and Zhang, W. (2019). Analysis of driving factors of photovoltaic power generation efficiency: a case study in China. *Energies* 12, 355. doi:10.3390/en12030355

Yue, X., Tang, Q., Xu, W., Zhao, X., Chen, Y., Liu, Z., et al. (2024). A multi-factor spatio-temporal correlation analysis method for PV development potential estimation. *Renew. Energy* 223, 119962. doi:10.1016/j.renene.2024.119962

Yushchenko, A., De Bono, A., Chatenoux, B., Ray, N., and Giuliani, G. (2018). GIS-based assessment of photovoltaic (PV) and concentrated solar power (CSP) generation potential in West Africa. *Renew. Sustain. Energy Rev.* 81, 2088–2103. doi:10.1016/j.rser.2017.06.021

Zhang, J., and Peng, S. (2024). Daily-scale 4 km gridded meteorological dataset for China (2000–2020). *Natl. Tibet. Plateau Data Cent*. doi:10.11888/Atmos.tpdc.301696

Zhang, Z., Li, R., Zhao, C., and Li, F. (2016). Cross-characterization of PV and sunshine profiles based on hierarchical classification. *Energy Procedia* 103, 15–21. doi:10.1016/j.egypro.2016.11.242

Zhang, K., Gann, D., Ross, M., Robertson, Q., Sarmiento, J., Santana, S., et al. (2019). Accuracy assessment of ASTER, SRTM, ALOS, and TDX DEMs for hispaniola and implications for mapping vulnerability to coastal flooding. *Remote Sens. Environ.* 225, 290–306. doi:10.1016/j.rse.2019.02.028

Zhang, L., Ren, Z., Chen, B., Gong, P., Fu, H., and Xu, B. (2024). Long-term annual artificial nightlight dataset for China (1984–2020). *Natl. Tibet. Plateau Data Cent*. doi:10.11888/Socioeco.tpdc.271202

Zhao, J., Wang, J., and Su, Z. (2014). Power generation and renewable potential in China. *Renew. Sustain. Energy Rev.* 40, 727–740. doi:10.1016/j.rser.2014.07.211

Zhao, X., Yue, X., Tian, C., Zhou, H., Wang, B., Chen, Y., et al. (2023). Multimodel ensemble projection of photovoltaic power potential in China by the 2060s. *Atmos. Ocean. Sci. Lett.* 16, 100403. doi:10.1016/j.aosl.2023.100403

Zhao, Y., Li, S., Yang, D., Chen, F., Wu, Y., and Liu, H. (2024). Assessment of site suitability for centralized photovoltaic power stations in Northwest China's six provinces. *J. Environ. Manag.* 366, 121820.